

Supporting Information

Half and Full Sodium-ion Batteries Based on Maize with High-loading Density and Long-cycle Life

Tingzhou Yang, Xiaoying Niu, Tao Qian,* Xiaowei Shen, Jingqiu Zhou, Na Xu, Zhouzhou Sun,
Chenglin Yan*

College of Physics, Optoelectronics and Energy & Collaborative Innovation Center of Suzhou Nano
Science and Technology, Soochow University, Suzhou 215006, China. Email: tqian@suda.edu.cn
(T. Qian); c.yan@suda.edu.cn (C. Yan).

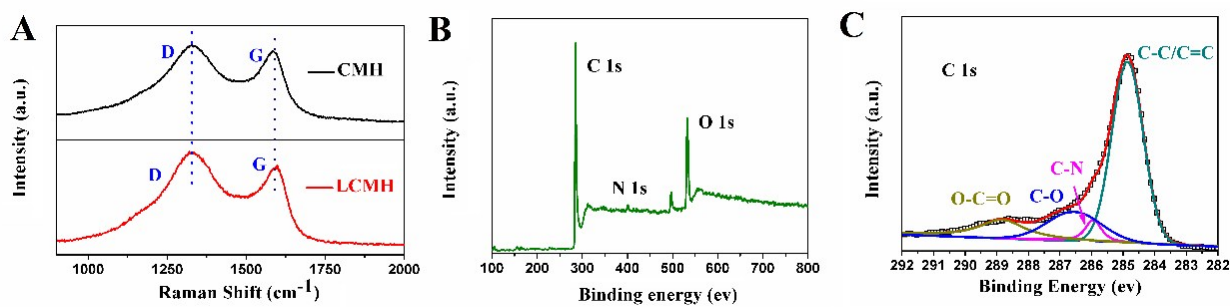


Figure S1. A) The Raman spectras of CMH and LCMH. B) From carefully analysis the X-ray photoelectron spectroscopy, the atomic percentage of C (77.48 at%), O (19.71 at%), and N (2.81 at%) can be reached, which the N produced by reduction reaction through ethylenediamine. C) It can be observed that the spectrum of C 1s is resolved into four components centered at 284.5, 285.8, 286.5 and 288.9 eV, corresponding to C-C/C=C, C-N, C-O and O-C=O, respectively.

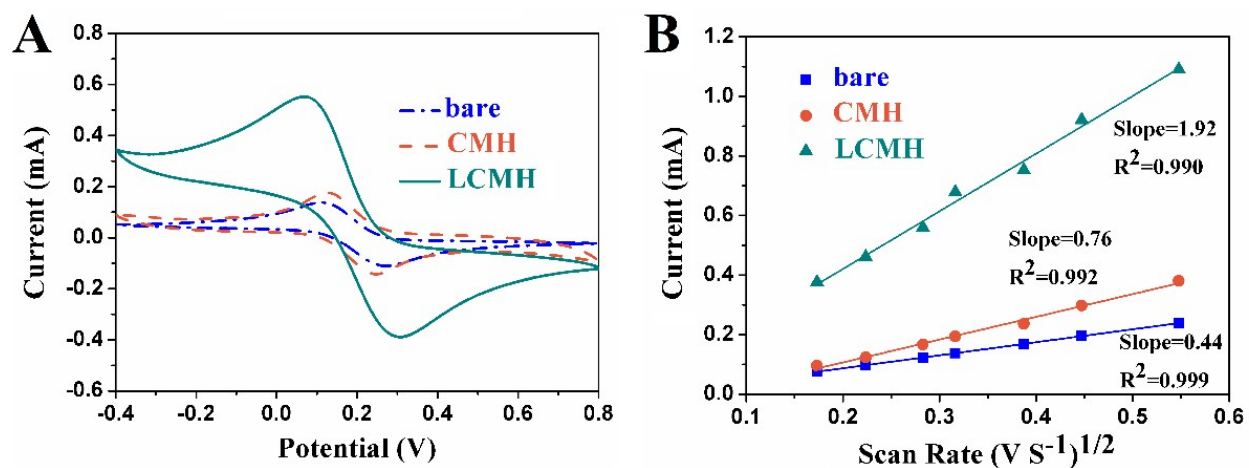


Figure S2. A) Cyclic voltammograms of bare GCE, CMH and LCMH modified GCE in a 10 mM $[Fe(CN)_6]^{3-/4-}$ and 100 mM KCl solution at a scan rate of $80\ mV\ s^{-1}$. B) Peak currents as a function of scan rates for the determination of the effective working surface area.

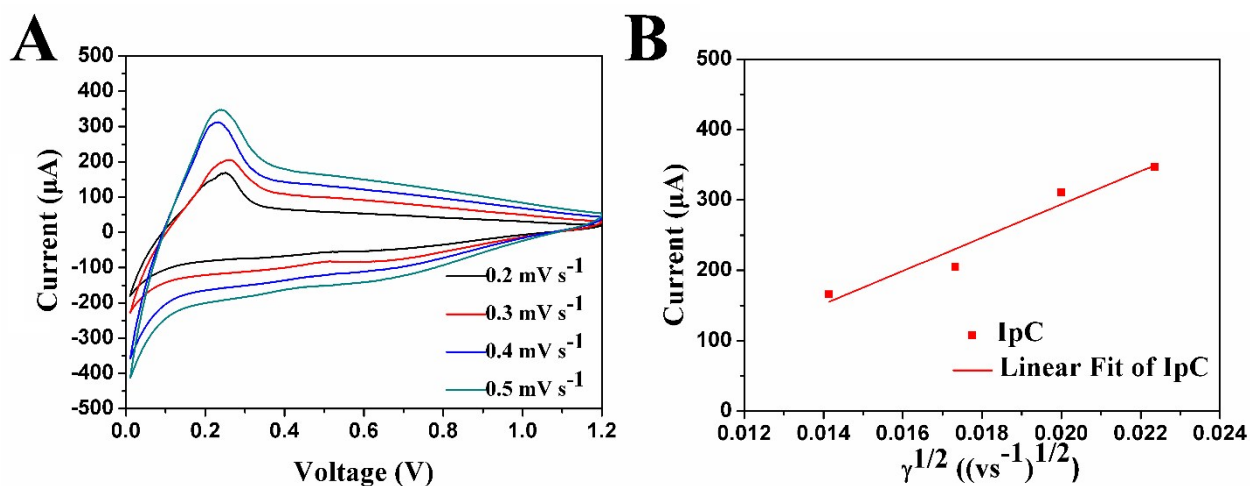


Figure S3. A) In order to further confirm the relationship between Na⁺ ion diffusion coefficients and high rate performance, CV tests of the half batteries at different scan rates from 0.2 to 0.5 mV s⁻¹ are displayed. B) The Randles-Sevcik equation is used to evaluate the Na⁺-ion diffusion coefficients (D_{Na}) of LCMH cathodes.

$$I_p = 2.69 \times 10^5 n^{3/2} A D_{\text{Na}}^{1/2} C_{\text{Na}} v^{1/2}$$

where v is the scan rate (V s^{-1}), D is the diffusion coefficient of Na ions, C_{Na} is the concentration of Na ions in the electrode (mol cm^{-3}), A is the surface area of the cathode, n is the number of electrons in reaction and I_p indicates the peak current. From the linear relationship of i_p and $v^{1/2}$, $D_{\text{Na}} = 5.21 \times 10^{-14} \text{ cm}^2 \text{ s}^{-1}$, which indicates that LCMH has a high Na⁺-ion diffusion coefficient.

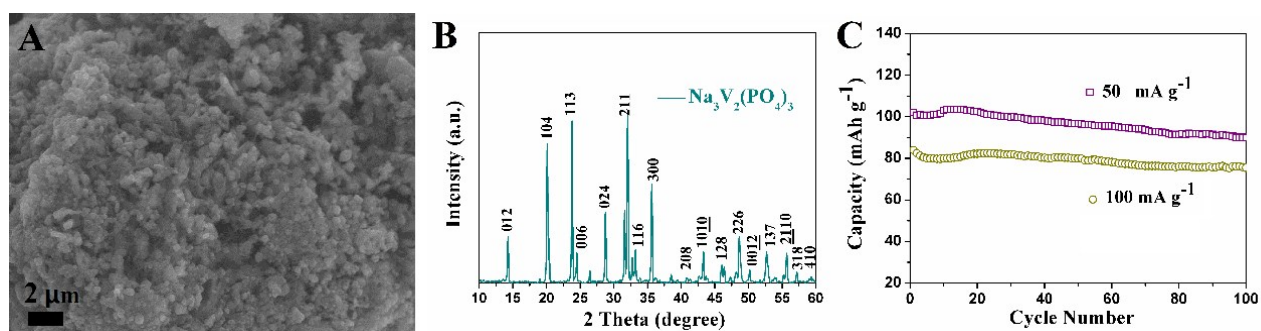


Figure S4. A) The SEM image of $\text{Na}_3\text{V}_2(\text{PO}_4)_3$, where the irregularly shaped particles are adhered to surface of the bulk production. B) From the X-ray diffraction (XRD) patterns of the final $\text{Na}_3\text{V}_2(\text{PO}_4)_3$ product, all of the diffraction peaks are indexed to the NASICON structure with the $R\bar{3}c$ space group (2 Na in 18e position, 1 Na in 6b position) and consistent well with previous work. C) Cycling performance of $\text{Na}_3\text{V}_2(\text{PO}_4)_3$ electrode at the current densities of 50 and $100\ \text{mA g}^{-1}$.

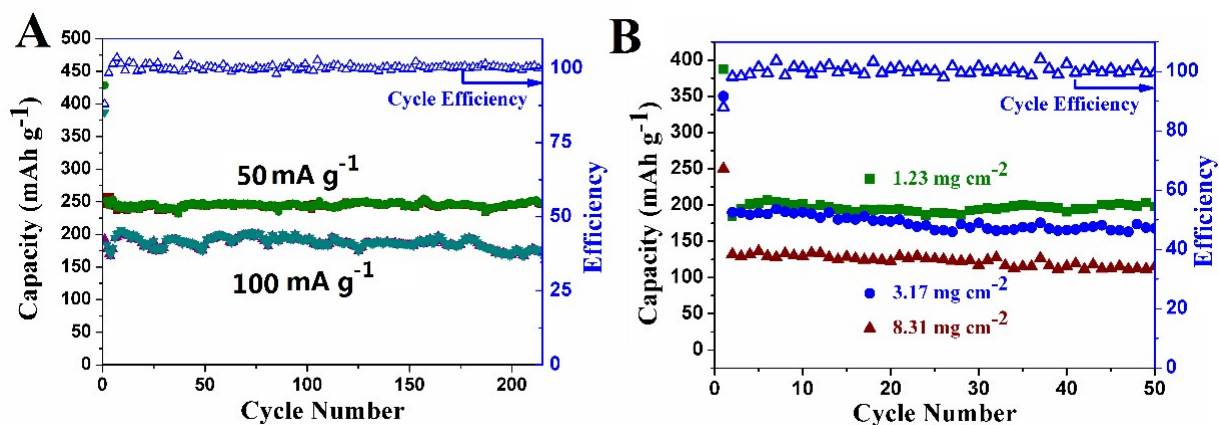


Figure S5. A) Reversible cycling capacity and coulombic efficiency over 200 cycles at different currents. B) The different cycling performance of different active material mass loading density, which is corresponding to Figure 4B.

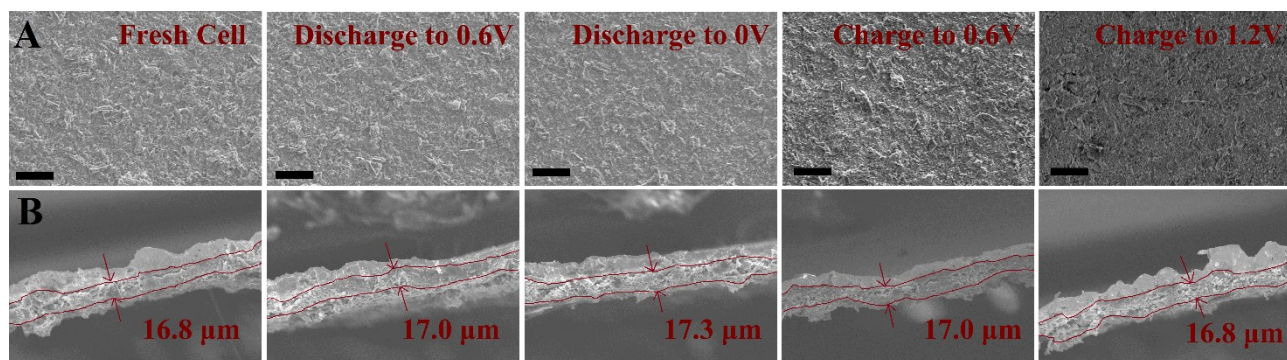


Figure S6. The A) morphologies and B) thickness of LCMH electrode during the different discharge and charge process are examined by SEM.

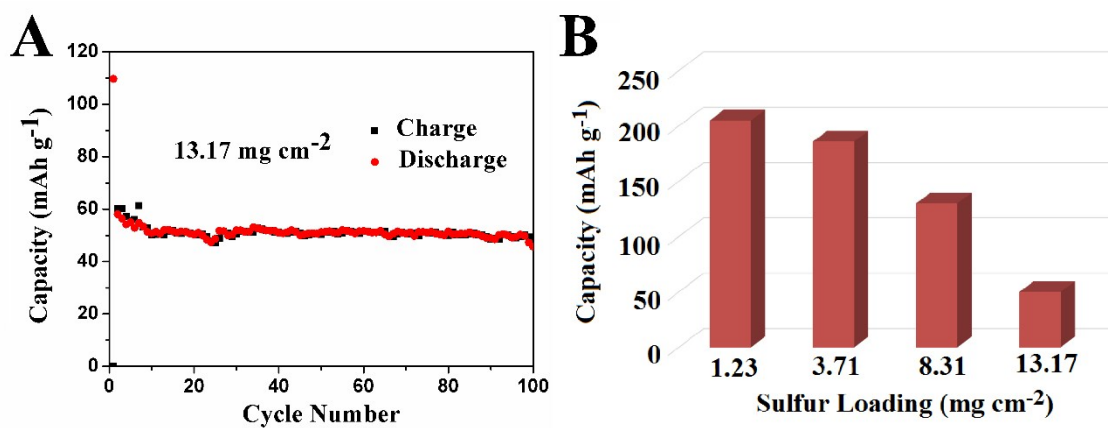


Figure S7. A) The cycling performance of mass loading up to 13.17 mg cm⁻². B) The capacity of LCMH is fading with an increase of the active material loading. A high loading up to 13.17 mg cm⁻² is revealed with low capacities of ~50 mA h g⁻¹.

Table S1. Kinetic parameters obtained from equivalent circuit fitting of experimental data from CMH and LCMH.

| | R_S (Ω) | R_{ct} (Ω) | R_f (Ω) |
|-------------|--------------------------|---------------------------|--------------------------|
| CMH | 3.42 | 12.9 | 126.3 |
| LCMH | 3.15 | 35.5 | 397.5 |